

Master thesis

Development of an HCCI index

TOVE VANG
FILIPPA OLSSON

Division of Combustion Engines
Department of Energy Sciences
Lund University
Lund 2009

Department of Energy Sciences
Faculty of Engineering
Lund University
SE-22100 Lund, Sweden

© Tove Vang and Filippa Olsson
ISRN LUTMDN/TMHP-09/5184-SE
ISSN 0282-1990
Printed in Sweden by Media-Tryck, Lund 2009

Acknowledgements

This master thesis has been conducted at the Division of Combustion Engines at Lund Institute of Technology.

We would like to thank our supervisor Dr Martin Tunér and Professor Bengt Johansson for all their help and support with our master thesis.

We would also like to thank our beloved engineers Kjell Jonholm, Bertil Andersson, Tommy Petersen and Tom Hademark. We have gotten more help and support than we could imagine from you. All of you have made this experience worthwhile for us.

Finally, we would like to thank our roommates, you know who you are, and the rest of the division for the wonderful atmosphere provided.

Abstract

New models of combustion engines have gained a great interest within research in the last decade. This interest has arisen due to the possibility to achieve a higher degree of efficiency and lower emissions, which will impact the environment positively. A higher degree of efficiency implicates an economical benefit in terms of fuel.

The HCCI engine has been thoroughly researched due to its combined advantages of the CI and SI engine. As always, there are disadvantages with this type of engine. The main problems are that the combustion is too quick and that the engine is difficult to control.

A good way to compare combustion of fuels in different engines is to develop a fuel index. In a fuel index data for mixtures are accounted for in a table, with which the index of an unknown fuel can be determined. In this master thesis only a limited number of fuels are tested, which means that a fully developed fuel index is not able to be accomplished without further research.

In this master thesis a fuel index for the HCCI engine has been partly determined by executing experimental and simulated studies. The fuels tested were Primary Reference Fuels 0 to 100. The engine has been run with inlet temperatures between 293 K and 423 K, in intervals of 10 K, and with a compression ratio that give 50 % burn at TDC. The HCCI engine was modeled and the simulations were performed in DARS, which is a chemical kinetics program.

The results from the simulations seem to be reasonable. The compression ratios and the ignition temperatures with the corresponding pressures are in the right magnitude. The results from the experiments, on the other hand, are not as reliable as the results from the simulations.

The model created in this master thesis may be used with an engine that has the same conditions as the simulations, if a more accurate chemical model is used and the indicator for the inlet temperature is placed at the correct location. Further research concerning the reason why the simulations and the experiments deviated is needed in order to be able to use this base for an index.

Contents

1. Introduction	1
1.1 Objective	1
1.2 Method	1
1.3 Constraints	2
2. The HCCI engine	3
2.1 The principle of the SI engine	3
2.2 The principle of the CI engine	4
2.3 The principle of the HCCI engine	4
2.4 Octane number	5
2.5 Combustion	6
2.6 Kinetics	6
3. Methods	9
3.1 The CFR engine	9
3.2 Experimental apparatus	9
3.3 Simulations with DARS	12
4. Results	23
4.1 Experimental results	23
4.2 Results from simulations	30
5. Conclusions	43
5.1 Discussion	43
5.2 Conclusions	45
6. References	47

1. Introduction

New models of combustion engines have gained a great interest within research in the last decade. This interest has arisen due to the possibility to achieve a higher degree of efficiency and lower emissions, which will impact the environment positively. A higher degree of efficiency implicates an economical benefit in terms of fuel.

Today the most common engines are the spark ignition, SI, and the compression ignition, CI. The SI has a lower efficiency as well as a lower emission level than the CI engine. The Homogenous Charge Compression Ignition, HCCI, engine combines the advantages of these engines which results in a low emission level and high efficiency. Research and development of this type of engine is a way to decrease harmful emissions. As always, there are disadvantages also with this type of engine. The main problems are that the combustion is too quick and that the engine is difficult to control.

A good way to compare combustion of fuels in different engines is to develop a fuel index. In a fuel index data for mixtures are accounted for in a table, with which the index of an unknown fuel can be determined.

1.1 Objective

Fuels today are classified with octane numbers for the SI engine and with cetane numbers for the CI engine. The objective of this master thesis is to partly develop a fuel index for the HCCI engine by executing experimental and simulated studies. To define an HCCI fuel index several different fuels must be tested. In this master thesis a limited number of fuels are studied, which is a start in the work of developing an HCCI index. The fuels tested are Primary Reference Fuels 0 to 100, in intervals of 10, where the number represents the percentage of n-heptane in an n-heptane/iso-octane mixture. The experiments, as well as the simulations, will be executed with inlet temperatures between 293 K and 423 K, in intervals of 10 K, and with a compression ratio that give 50 % burn at TDC. In this master thesis only a limited number of fuels are tested, which means that a fully developed fuel index is not able to be accomplished without further research.

1.2 Method

The experimental study is executed on a CFR engine in HCCI mode. A LabView control program collects data from the engine, which is then processed in a Matlab program. The simulations are

performed in DARS, which is a chemical kinetics program. With this program a model for the HCCI engine is developed in three steps, which is then used in the simulations.

1.3 Constraints

In this master thesis only a limited number of reference fuels are tested. In the simulation program the chemistry model used is reduced and consists of only 38 reactions, which will affect the accuracy of the results. The number of experiments is time limited, which may affect the reliability of the results. The amount of residual gases in the engine is unknown, which might affect the simulated results slightly. The residual gases usually lie around 10 to 15 percent and are therefore set to 10 percent in the simulations.

2. The HCCI engine

The HCCI engine performs almost like a combination of the SI and the CI engine. In the following subchapters these engines are explained to give a better understanding to the subject of this master thesis.

2.1 The principle of the SI engine

The SI engine can have either a two stroke or a four stroke cycle. A stroke is when the piston moves from the bottom to the top or vice versa.

In a two stroke cycle, air or an air-fuel mixture fills the cylinder and the compression takes place when the piston moves upwards. The combustion, which leads to an increase in pressure, starts right before the piston reaches the top. The mixture is ignited by a spark, causing a flame to burn and propagate through the fuel. The expansion takes place when the piston is at the top; the piston is then pressed downwards. When the piston reaches the Top Dead Center, TDC, part of the exhaust gases are depleted, which leads to a pressure drop. The cylinder is then filled with inlet gases simultaneously as it is depleted of excess gases.

A four stroke cycle, see figure 2.1, begins with a stroke where air or an air-fuel mixture fills the cylinder. During the second stroke the compression occurs and when the mixture has been ignited by a spark at the end of the stroke, the combustion starts. Expansion occurs throughout the third stroke and towards the end; part of the exhaust gases are depleted in order to lower the pressure. The cylinder is depleted of excess gases during the fourth stroke.

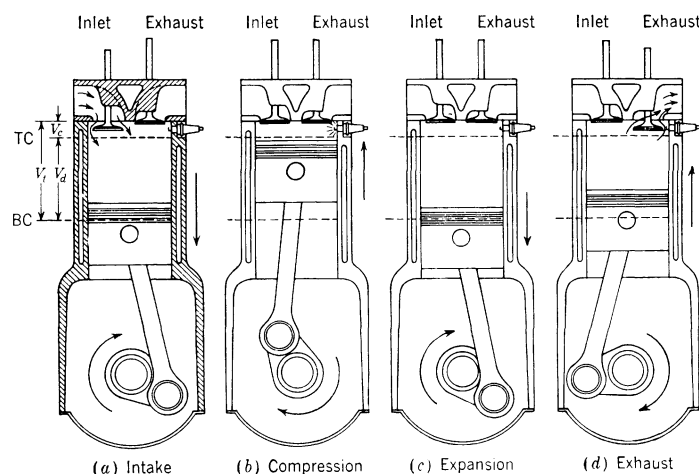


Figure 2.1 The four stroke cycle [1]

The stoichiometric relation between air and fuel is the best relation to use in this case since all oxygen and fuel is consumed. Other relations between fuel and air give poorer combustion. If the air-fuel mixture is surplus heated before it ignites, knocking, i.e. auto-ignition may occur. When knocking takes place the mixture is combusted in a very short time, which may lead to damages on the engine. [1]

2.2 The principle of the CI engine

In a CI engine the cylinder is filled with merely air during the first stroke. Compression occurs at a high compression ratio throughout the second stroke, during which the air is heated to a large extent. At the end of the compression stroke the fuel is injected at high pressure and then it atomizes, vaporizes and mixes partially before auto-ignition takes place. The mixed part is combusted rapidly and during the rest of the combustion fuel is injected, atomized, mixed and combusted continuously in an almost constant rate.

The CI engine has higher efficiency than the SI engine due to higher compression ratio. Disadvantages with the CI engine are the expensive injection system and emissions in the form of soot and NO_x , which is formed at high temperatures with oxygen present. Most of the NO_x emissions are formed in the premixed part of the combustion blend. Soot forms when there is a shortage of oxygen, primarily in the non-premixed parts. [1]

2.3 The principle of the HCCI engine

In the HCCI engine an air-fuel mixture enters the cylinder, which is identical to the procedure in the SI engine. As with the CI engine, the mixture auto-ignites due to the large amount of heat which develops during compression. The combustion however, differs from that of the two other engines. The combustion initiates simultaneously at several points in the cylinder. There is no flame propagation in the HCCI engine, as it is in the SI engine; instead the fuel burns almost at the same time.

For the mixture to auto-ignite a high compression ratio or preheating of the mixture is needed. If the mixture is to be ignited at a certain crank angle degree a specific combination of inlet temperature, inlet pressure and compression ratio is required.

The HCCI engine performs simply when the combustion starts at the right time. Too fast fuel consumption is a problem which may arise while running the engine. This will occur if the fuel is

not diluted, as it is for an SI engine. Dilution of a fuel can be achieved by using excess air or Exhaust Gas Recirculation, EGR. The rich limit for λ is 2.2 and if a lower value of λ is used a large part of the exhaust gases has to be recirculated. The engine ought to be run at homogenous conditions in order to decrease the amount of rich zones. The advantages with the HCCI engine are its low emission level and high efficiency. [1]

2.4 Octane number

The octane number indicates a fuel's resistance to knocking. To obtain this number a standardized engine with "variable" compression is operated with two different reference fuels, iso-octane and n-heptane. The latter, which has low resistance to knocking, is given the number 0 and iso-octane, which has high resistance to knocking, is given the number 100.

To determine the test fuel's octane number the data is compared to two reference fuels, which consist of one fuel with a higher and one with a lower octane number than the test fuel. The octane number is linear with the compression ratio for the reference fuels.

There are two different octane numbers, RON and MON. At the determination of the octane number with the RON-method the engine is run at 600 rpm, the inlet air temperature is 52°C, the ignition angle is constant and λ is set at maximal knocking. With the MON-method the engine is run at 900 rpm, the inlet air temperature is 149°C and the ignition angle varies slightly with the compression ratio. The octane number from the RON and MON method is the same for iso-octane and n-heptane but generally MON gives a lower value than RON.

The octane number for the SI engine may be used with the HCCI engine, but it is important to have in mind that a small error may occur when using the octane number for the HCCI engine.

For CI engines a cetane number is used instead of an octane number. The reference fuels used are cetane, with a cetane number of 100, and α -methyl-naphthalene, with a cetane number of 0. Due to the latter fuel's instability, heptamethylnonane, with a cetane number of 15, is used instead. The octane number, ON, and the cetane number, CN, are related according to equation (2.1). [1]

$$ON = 120 - 2 \times CN \quad (2.1)$$

The sensitivity to knocking is not the same for all kinds of engines. Therefore an index such as the ON and CN is a good way to know if a fuel is suitable to a certain engine. When running an engine, the ON or CN interval at which a fuel may be used, as well as the kind of fuel that is suitable, is specific.

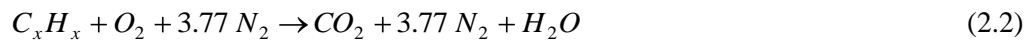
2.5 Combustion

The combustion process occurs in a chamber after the combustion has been initiated. For the combustion to take place oxidizer and fuel is needed. The fuel may be solid, liquid or gaseous and the oxidizer used is often air, which besides oxygen consist of incombustible nitrogen and traces of other gases.

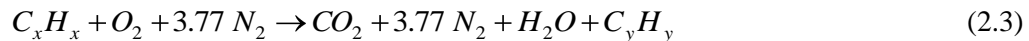
Excess oxygen is used to ensure total combustion. The fuel mixture is referred to as lean if there is a surplus of oxygen, but if there is not enough oxygen the mixture is referred to as rich. As mentioned in chapter 2.3 the fuel mixture has to be rich in order to run the engine in HCCI mode.

When the combustion has occurred, the exhaust gases along with the incombustibles and any excess oxygen are depleted from the chamber.

Equation (2.2) below is the reaction formula for ideal combustion.



In reality this process is most likely not ideal, hence hydrocarbons will be produced according to equation (2.3). [2]



2.6 Kinetics

Kinetics is important to understand when simulating chemical reactions, therefore the basics are explained in this chapter.

The general definition of the reaction rate is the rate at which products are formed. The reaction rate depends on concentration and temperature. A general formula of a reaction is shown below,

where ν is the symbol for the stoichiometric coefficient. The letters A and B are the reactants and C and D are the products.



There are three different ways to define the rate at which the reaction occurs. These are the rate of formation for a specific component (r_x), the consumption rate for a component and the conversion rate of the formula (r). The conversion rate of the formula specifies the direction of the reaction, which is positive for a forward reaction (from left to right). The rate of formation, as well as the stoichiometric coefficient, is positive for products, negative for reactants and zero for inert components. The relation between these two parameters is shown in equation (2.5).

$$r_x = \nu_x \times r \quad (2.5)$$

To describe the consumption of a specific component the conversion variable is used. This variable is defined as in equation (2.6) below and its value lies between zero and one. The parameter n_x is the number of moles of the component X.

$$x_x = \frac{n_{x0} - n_x}{n_{x0}} \quad \text{mole X converted / mole X from the beginning} \quad (2.6)$$

The reaction rate may be of different orders. The equation for the conversion rate of the formula may be as shown in equation (2.7), where y is an integer and k is the reaction rate constant.

$$r = k \times C_X^y \quad (2.7)$$

The Arrhenius relation below is used to estimate the reaction rate constant, k . In the equation E_A is the activation energy, R is the ideal gas constant and k_0 is a specific constant.

$$k = k_0 \times e^{-E_A/(R \times T)} \quad (2.8)$$

The expression for the conversion rate of the formula and the reaction rate order is determined through experimental studies. [3]

3. Methods

In this chapter the methods used in the experiments and in the simulations are explained in details. The model used in the simulations is being built-up in three steps and the results, in order of compression ratio and ignition pressure, are compared to each other.

3.1 The CFR engine

The CFR, The Cooperative Fuel Research, established test engine methods for rating of fuels in the late 1920's. In 1931 the CFR engine, which is a standardized single cylinder engine, was developed and it is produced by Waukesha Motor Company. The reference fuels were n-heptane and iso-octane and the fuel index reaching from 0 to 100 was developed. In the same year the standardized test method RON, Research Octane Number, was established. Later the standardized test method MON, Motor Octane Number, was developed. The MON and RON method was explained in chapter 2.4. Today the engine is operated with either the MON or the RON method. [4]

3.2 Experimental apparatus

The engine used in the experiments for this master thesis is a CFR engine which will be run in HCCI mode. The engine is new but it is built after a model from the 1930's. The engine is shown in figure 3.1.



Figure 3.1 The CFR engine

A control program made in Lab View is used to collect data from the engine. The interface is shown in figure 3.2.

In the interface the output values from the engine, as well as the pressure trace along with the heat release, are shown. When starting the engine the compression ratio and the injection flow are set to that of an SI engine. To change into HCCI mode the compression ratio is increased and the injection flow is decreased until the desired pressure profile and lambda are achieved. To measure lambda a lambda sensor is used, which can be compared to the calculated value from the control program.

Emission equipment is used to obtain the correct lambda value and it is also used to determine the extent of the combustion.

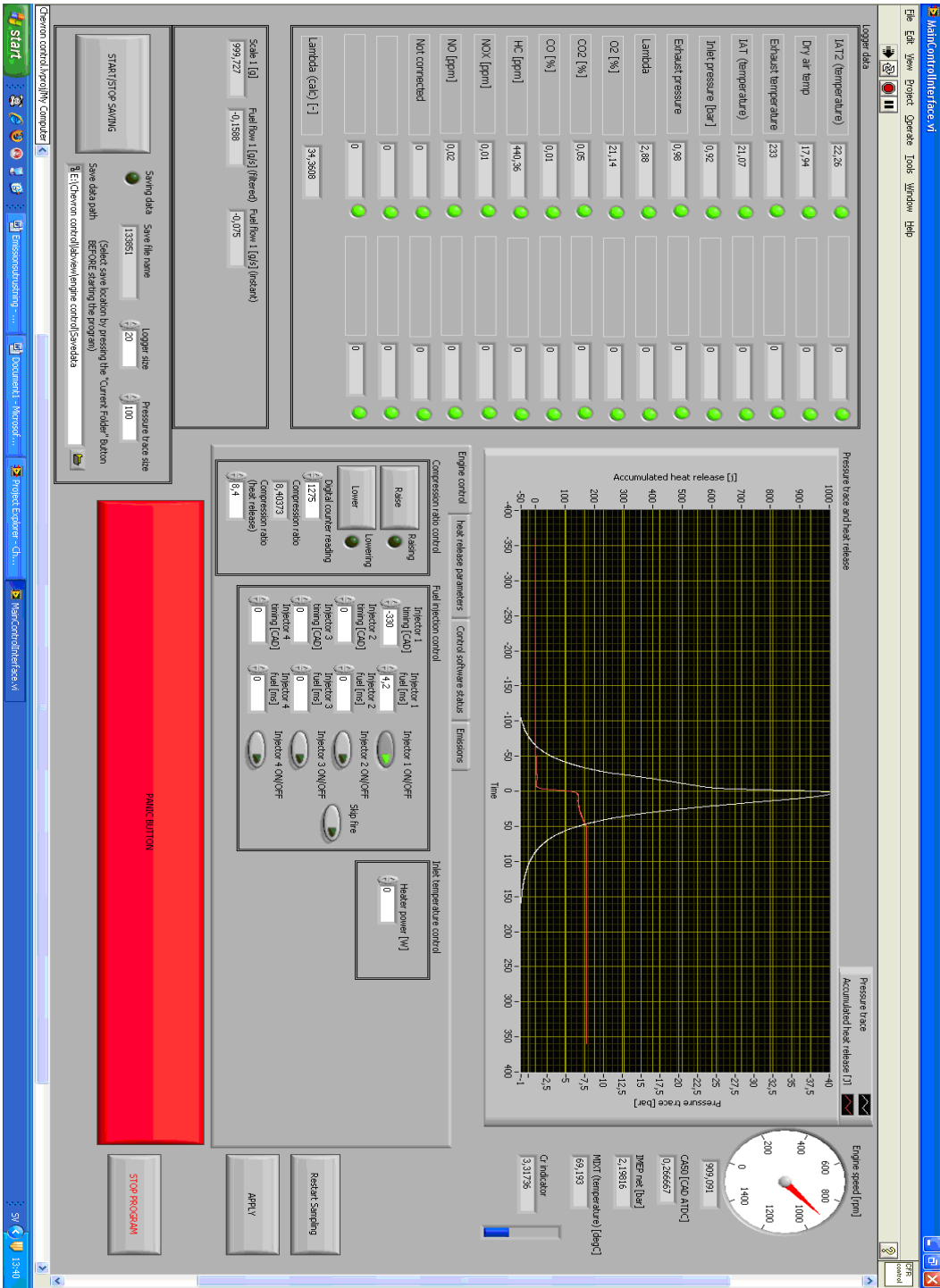


Figure 3.2 The interface of the control program made in LabView

The constant data for the engine that is used in the simulation program is found in table 3.1 below.

Table 3.1 Constant data for the HCCI engine

Parameter	Value
Stroke (m)	114.3×10^{-3}
Bore (m)	82.6×10^{-3}
Connecting rod length (m)	254×10^{-3}
Initial crank angle degree (TDC)	-180
Final crank angle degree (TDC)	180 (0)
Engine Speed (RPM)	900
λ (experiments and simulations)	3
A_{p0} (chamber head area/piston area)	1.02
Inlet pressure (experiments, bar)	1.5

3.3 Simulations with DARS

DARS is a chemical kinetics program. The program is used for simulation of different engines, e.g. the HCCI engine. Data for different components and chemical reactions may be inserted in the program.

The simulations in this master thesis are executed with the help of a reduced chemistry model consisting of 38 reactions. [5]

The model will be built-up in small steps. The ideal model will be simulated first and then the heat exchange will be added. Last the recirculated exhaust gas together with the residual gases will be added. The gases are labeled EGR in the simulation program; therefore they are labeled the same in this master thesis. This creates a more realistic model that will correspond to the real engine. To simulate the model the relations below are used.

The general heat exchange equation is given in equation (3.1).

$$Q = A \times h \times \Delta T \quad (3.1)$$

The heat-transfer coefficient, h , will be modeled with the Woschni equation below. [6]

$$h_c(W/m^2 \times K) = 3.26B(m)^{-0.2} \times p(kPa)^{0.8} \times T(K)^{-0.55} \times w(m/s)^{0.8} \quad (3.2)$$

$$w = \left[C_1 S_p + C_2 \frac{V_d T_r}{P_r V_r} (p - p_m) \right] \quad (3.3)$$

The engine speed is set to 900 rpm and the tolerance limit for the simulations is 10^{-10} .

From the simulations the ignition temperature and pressure is obtained, see figures 3.3 – 3.4. The ignition temperature is defined as the temperature at 1 Crank Angle Degree before 1 percent of the heat release.

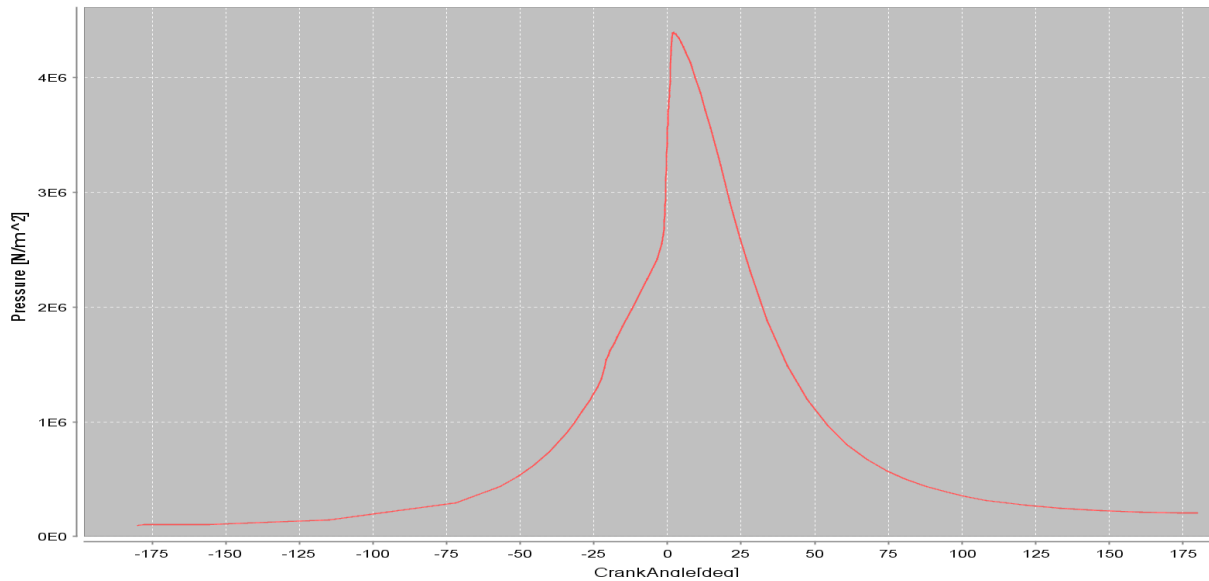


Figure 3.3 The pressure simulated in DARS

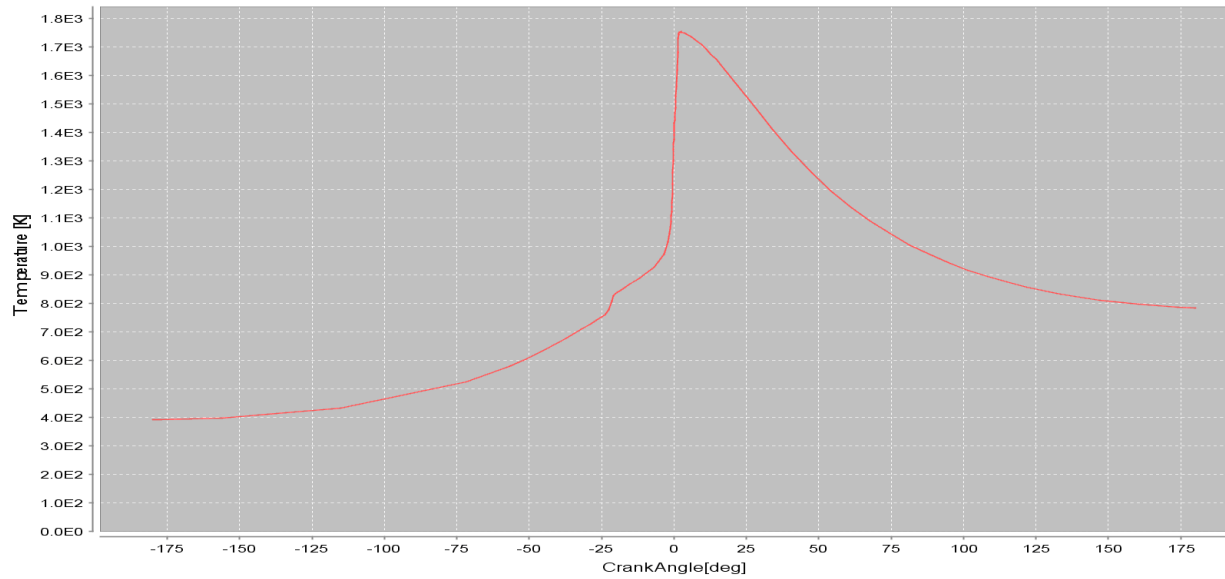


Figure 3.4 The temperature simulated in DARS

The results from the ideal model simulated with PRF 0, i.e. 100 % n-heptane, are shown in table 3.2. In the table the Crank Angle Degree, CAD, displayed is 1 CAD before 1 percent of the heat release. The ignition temperature and its corresponding pressure are found at a specific CAD. These results, along with the compression ratio, are shown in the tables.

The data is plotted in Matlab, see figure 3.5. It is plotted in this way to help determine the octane number for fuels that are not reference fuels. In figure 3.5, the inlet temperature of 423 K is represented by the curve furthest to the left and the inlet temperature decreases by 10 K for each curve further to the right. This applies to all figures of the same type in this master thesis.

Between PRF 0 and PRF 90 there will be a wave in the graph that is not seen in PRF 100. The size of the wave decreases with the amount of n-heptane in the mixture. The wave gives an indication of the amount of cool flame combustion present.

Table 3.2 Results for the ideal model with PRF 0

Inlet gas temperature (K)	Compression ratio	Temperature (K)	Pressure (bar)	CAD
293	13.67	956	46.16	-1.53
303	12.64	963	41.60	-1.51
313	11.73	966	37.49	-1.53
323	10.93	968	33.91	-1.61
333	10.23	974	30.99	-1.66
343	9.60	976	28.28	-1.74
353	9.04	983	26.08	-1.76
363	8.54	990	24.12	-1.76
373	8.10	997	22.43	-1.64
383	7.71	997	20.79	-1.82
393	7.36	1006	19.52	-1.81
403	7.05	1016	18.43	-1.71
413	6.77	1029	17.50	-1.55
423	6.49	1016	16.16	-1.36

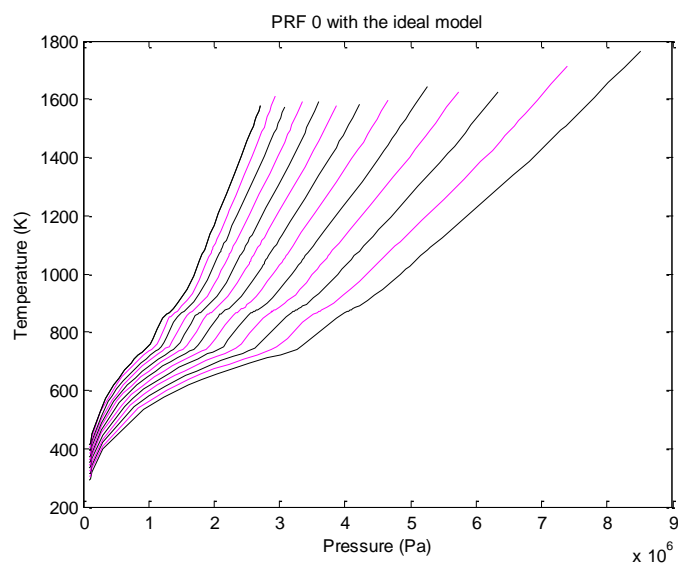


Figure 3.5 The results for the ideal model simulated with PRF 0

The ideal model with added heat exchange is presented next. In order to do this the following facts are needed.

The constants C_1 and C_2 are set to 2.28 and 0.0 respectively. [6] The wall temperature is usually between 423 K and 473 K [7] and is set to 448 K in the simulations. The relation between the chamber head area and the piston area, A_{p0} , is 1.02. The simulations will be done for PRF 0 with an inlet temperature between 293 K and 423 K set in steps of 10 K and with a compression ratio adjusted to keep 50 % burn at TDC.

The results for PRF 0 with heat transfer but without recirculation are shown in table 3.3. The data is plotted in Matlab, see figure 3.6.

Table 3.3 Results for the ideal model with heat transfer with PRF 0.

Inlet gas temperature (K)	Compression ratio	Temperature (K)	Pressure (bar)	CAD
293	13.28	960	45.08	-1.50
303	12.40	959	40.61	-1.62
313	11.62	967	37.17	-1.61
323	10.93	967	33.88	-1.78
333	10.30	970	31.06	-1.82
343	9.74	982	28.90	-1.80
353	9.22	982	26.56	-1.82
363	8.74	989	24.70	-1.41
373	8.35	993	23.05	-1.54
383	7.98	995	21.50	-1.54
393	7.66	999	20.19	-1.57
403	7.38	1005	19.07	-1.74
413	7.11	1012	18.06	-1.55
423	6.88	1015	17.11	-1.55

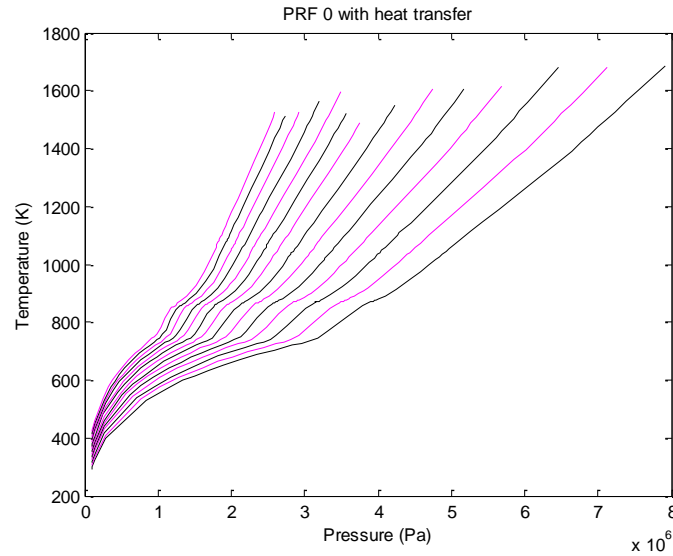


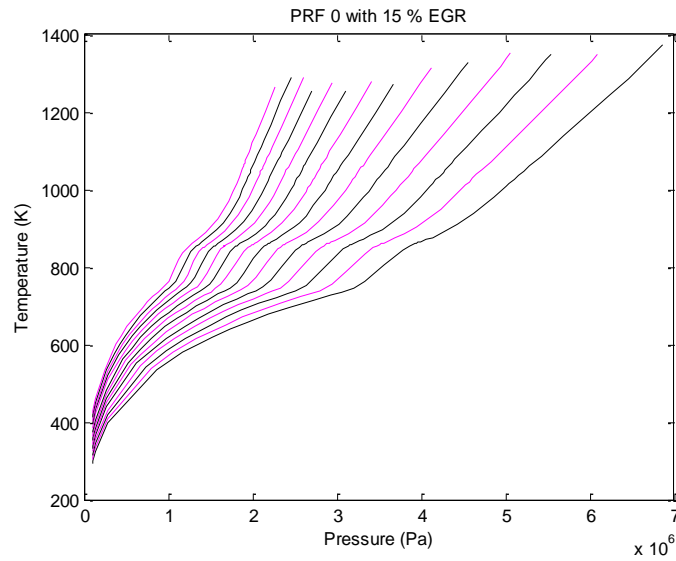
Figure 3.6 The results for the almost ideal model containing heat transfer simulated with PRF 0

Last of all the EGR, which usually lies around 10 % to 15 %, will be added. The simulations will be done with 10 % and 15 % exhaust gas recirculation, for PRF 0, and the number of EGR cycles is set to 5. The EGR is set to 10 % in the other simulations. The heat transfer will be set as previously. The simulations will be done for PRF 0 with an inlet temperature between 293 K and 423 K set in steps of 10 K and with a compression ratio adjusted to keep 50 % burn at TDC.

The results from the model with heat transfer and 15 % EGR simulated with PRF 0 are shown in table 3.4. The data is plotted in Matlab, see figure 3.7.

Table 3.4 Results for PRF 0 with heat transfer and 15 % EGR

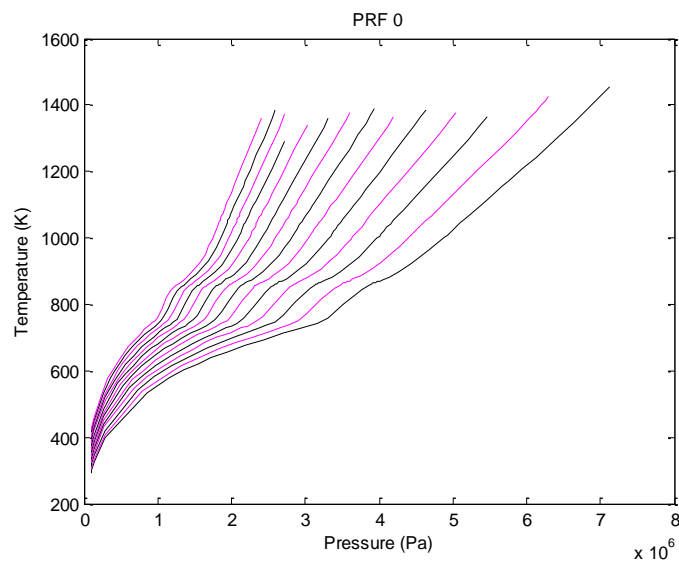
Inlet gas temperature (K)	Compression ratio	Ignition temperature (K)	Ignition pressure (bar)	CAD
293	14.05	954	47.10	-1.98
303	13.10	953	42.45	-1.89
313	12.30	967	39.20	-1.81
323	11.57	961	35.48	-2.04
333	10.90	971	32.80	-1.85
343	10.28	980	30.33	-1.62
353	9.75	980	27.95	-1.66
363	9.27	987	26.03	-1.66
373	8.84	989	24.22	-1.64
383	8.45	994	22.65	-1.58
393	8.11	1002	21.37	-1.56
403	7.79	1003	20.04	-1.55
413	7.52	1006	18.93	-1.56
423	7.27	1011	17.95	-1.51

**Figure 3.7 The results for PRF 0 with 15 % EGR**

The results from the model with heat transfer and 10 % EGR simulated with PRF 0 are shown in table 3.5. The data is plotted in Matlab, see figure 3.8.

Table 3.5 The results for PRF 0, i.e. 10 % EGR

Inlet gas temperature (K)	Compression ratio	Ignition temperature (K)	Ignition pressure (bar)	CAD
293	13.78	971	47.17	-1.53
303	12.85	959	41.98	-1.75
313	12.00	966	38.24	-1.56
323	11.30	960	34.67	-1.85
333	10.66	966	31.93	-1.83
343	10.07	972	29.48	-1.72
353	9.57	984	27.56	-1.72
363	9.09	981	25.39	-1.79
373	8.67	989	23.77	-1.70
383	8.27	993	22.18	-1.51
393	7.92	1002	20.90	-1.23
403	7.65	1004	19.70	-1.63
413	7.39	1011	18.70	-1.69
423	7.13	1011	17.64	-1.49

**Figure 3.8 The results for PRF 0**

The following simulations are done with the latter model with 10 % EGR, which is the most realistic of the three models used.

The simulated models are compared with each other in figures 3.9 – 3.10 below. The ideal model is represented by the magenta curve, the almost ideal model with heat transfer is represented by the black curve and the model with 10 % EGR is represented by the green curve.

In figure 3.9 below, the magenta curve differs in shape from the other two curves, which are almost parallel. The ignition pressure is higher for the model with 10 % EGR, with even higher pressures at lower temperatures, than for the half-ideal model due to volume changes.

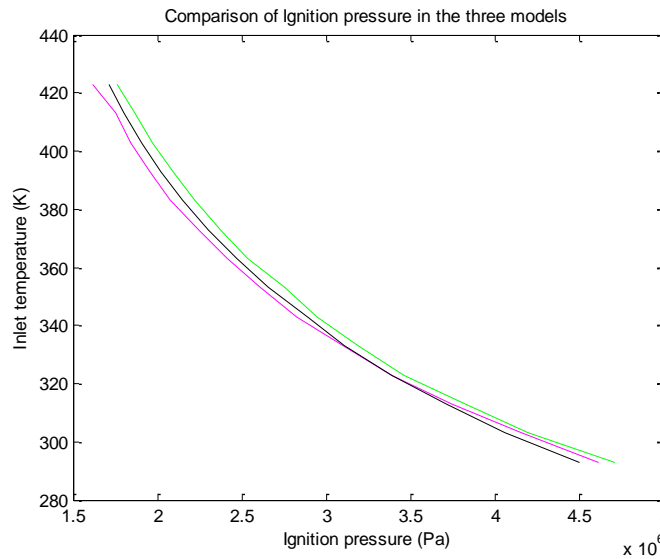


Figure 3.9 Comparison of the simulated ignition pressure of the three models

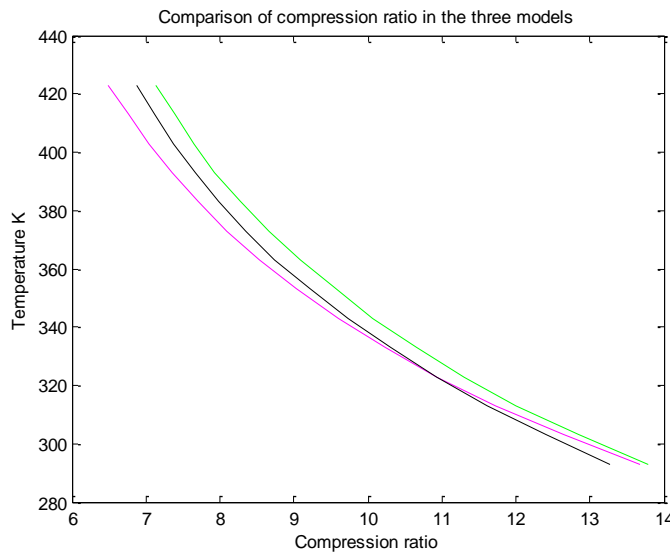


Figure 3.10 Comparison of the simulated compression ratio of the three models

In figure 3.10 above, the magenta curve differs in shape from the other two curves, which are almost parallel. The compression ratio is higher for the model with 10 % EGR, with a slightly higher compression ratio at lower temperatures, than for the half-ideal model due to volume changes.

The simulated models with 10 % EGR and 15 % EGR are compared with each other in figures 12 – 13 below. The model with 10 % EGR is represented by the black curve and the model with 15 % EGR is represented by the magenta curve.

For the ignition pressure, figure 3.11, the curves are parallel to a certain extent but at the highest and the lowest temperatures the curves narrow off. As seen in table 3.4 – 3.5 the ignition pressure is almost the same despite the difference in EGR. Regarding the compression ratio, there is a small difference in the simulated results; the compression ratio is slightly higher with 15 % EGR than with 10 % EGR, which can be seen in figure 3.12 below.

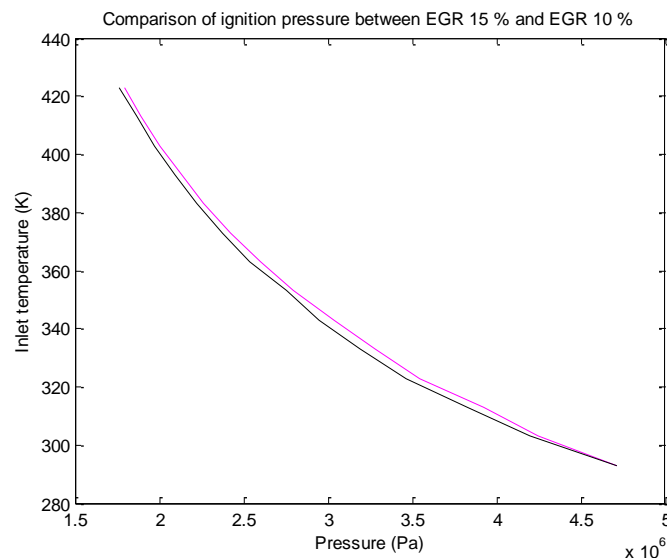


Figure 3.11 Comparison of the simulated ignition pressure between EGR 15 % and EGR 10 %

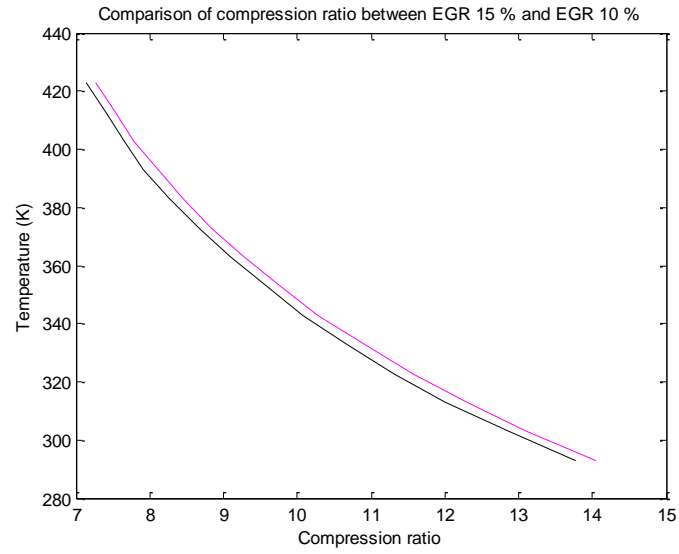


Figure 3.12 Comparison of the simulated compression ratio between EGR 15 % and EGR 10 %

4. Results

The results from the experiments and the simulations are presented in figures and tables in this chapter. The raw data from the experiments are found in appendix A.

4.1 Experimental results

Between two and six experiments were done per inlet temperature and PRF. The experiments were performed on the CFR engine with one temperature at a time, starting with PRF 0. The useful results obtained via the control program were the pressure trace for the whole cycle. To convert the pressure trace to heat release a Matlab program was used. With the new data the ignition pressure, i.e. the pressure at 1 CAD before 1 percent of the heat release, was obtained. The data was assumed to be linear; therefore interpolation of the ignition pressure and the compression ratio was done to get the same CAD, -1.00, for a better comparison of the data obtained. This was done due to the large variation in CAD in the data from the experiments.

The compression ratio is calculated with equation (4.1) in the control program.

$$CR = \frac{6345}{2132 - DCR} + 1 \quad (4.1)$$

This equation gives an incorrect value of the compression ratio. To determine the correct value the engine was run without combustion for a number of digital counter readings, DCR. The correct compression ratio was then determined by using equation (4.2).

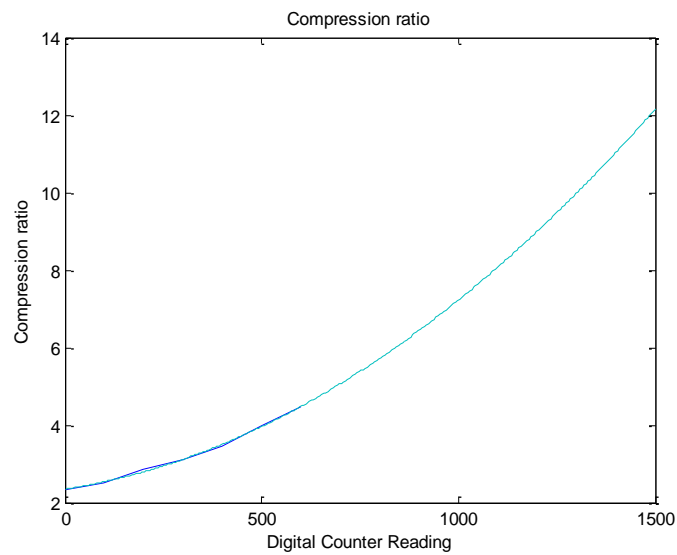
$$CR = \left(\frac{P_{\max}}{P_{\text{intake valve close}}} \right)^{\left(\frac{1}{1.36} \right)} \quad (4.2)$$

The compression ratios obtained were plotted and the data was interpolated, as seen in figure 4.1. By calculating the DCR, with equation (4.1), from the experimental compression ratios the correct value was obtained by using figure 4.1.

In table 4.1 data from the calculations of the compression ratios is shown.

Table 4.1 Data from the calculations of compression ratios

DCR	P_{max} (bar)	P_{intake valve close} (bar)	CR
0	9.2	2.87	2.35
100	9.47	2.71	2.51
200	9.53	2.29	2.85
300	9.88	2.11	3.11
400	10.27	1.90	3.46
500	10.70	1.63	3.99
600	11.38	1.48	4.48

**Figure 4.1 The variation of the calculated experimental compression ratio with the DCR**

In the experiments, the lowest inlet gas temperature obtained was 303 K and therefore the inlet temperatures 293 K and 303 K could only be simulated in DARS. The fuel PRF 100 was not able to be run due to its too high compression ratio.

Table 4.2 Experimental results for PRF 0

Inlet gas temperature (K)	Compression ratio	Calculated compression ratio	Calculated DCR	Pressure (bar)	CAD
313	7.47	8.56	1151	25.65	-1.00
323	7.40	8.45	1140	22.90	-1.00
333	7.54	8.65	1161	23.68	-1.00
343	7.71	8.86	1186	25.38	-1.00
353	7.33	8.35	1129	24.35	-1.00
363	6.75	7.48	1028	28.57	-1.00
373	6.77	7.49	1032	30.62	-1.00
383	6.74	7.46	1026	25.80	-1.00
393	6.24	6.62	921	22.50	-1.00
403	6.20	6.55	912	24.38	-1.00
413	6.34	6.80	944	23.05	-1.00
423	5.86	5.92	826	23.07	-1.00

Table 4.3 Experimental results for PRF 10

Inlet gas temperature (K)	Compression ratio	Calculated compression ratio	Calculated DCR	Pressure (bar)	CAD
313	7.71	8.87	1186	27.62	-1.00
323	6.50	7.10	978	21.15	-1.00
333	6.63	7.27	1005	21.34	-1.00
343	7.14	8.10	1098	27.15	-1.00
353	7.34	8.37	1131	25.39	-1.00
363	7.23	8.22	1113	24.77	-1.00
373	6.72	7.43	1023	26.63	-1.00
383	6.76	7.47	1030	25.48	-1.00
393	6.47	7.02	972	23.50	-1.00
403	6.28	6.69	930	24.00	-1.00
413	6.21	6.58	914	24.29	-1.00
423	6.88	7.71	1053	23.62	-1.00

In table 4.3 the values for the inlet gas temperatures 313 K and 343 K differs from the expected values. These temperatures have been run several times but with unsatisfying results. The reason for this behavior is unknown.

Table 4.4 Experimental results for PRF 20

Inlet gas temperature (K)	Compression ratio	Calculated compression ratio	Calculated DCR	Pressure (bar)	CAD
313	6.75	7.48	1028	21.10	-1.00
323	6.67	7.35	1013	21.83	-1.00
333	7.01	7.85	1076	23.64	-1.00
343	6.61	7.25	1001	23.33	-1.00
353	7.13	8.06	1097	23.56	-1.00
363	6.94	7.55	1034	25.20	-1.00
373	6.92	7.76	1060	25.02	-1.00
383	6.72	7.43	1023	23.39	-1.00
393	6.78	7.55	1034	25.42	-1.00
403	6.29	6.72	932	23.53	-1.00
413	6.32	6.77	939	25.06	-1.00
423	6.17	6.50	905	25.12	-1.00

Table 4.5 Experimental results for PRF 30

Inlet gas temperature (K)	Compression ratio	Calculated compression ratio	Calculated DCR	Pressure (bar)	CAD
313	7.14	7.48	1098	22.83	-1.00
323	6.90	7.79	1056	22.23	-1.00
333	7.13	8.10	1097	23.06	-1.00
343	7.17	8.11	1103	25.02	-1.00
353	7.07	7.97	1086	25.03	-1.00
363	7.41	8.49	1142	25.26	-1.00
373	6.96	7.81	1067	22.87	-1.00
383	6.73	7.46	1024	25.88	-1.00
393	6.71	7.43	1021	26.06	-1.00
403	6.62	7.28	1003	24.59	-1.00
413	6.61	7.27	1001	27.29	-1.00
423	6.53	7.17	984	27.60	-1.00

Table 4.6 Experimental results for PRF 40

Inlet gas temperature (K)	Compression ratio	Calculated compression ratio	Calculated DCR	Pressure (bar)	CAD
313	7.28	7.42	1121	23.25	-1.00
323	7.48	8.54	1153	24.14	-1.00
333	7.17	8.11	1103	23.20	-1.00
343	7.21	8.22	1110	22.67	-1.00
353	7.30	8.32	1125	24.32	-1.00
363	7.79	8.97	1197	26.25	-1.00
373	7.33	8.35	1129	26.66	-1.00
383	7.40	8.45	1140	28.62	-1.00
393	7.56	8.69	1165	29.90	-1.00
403	7.04	7.95	1081	29.70	-1.00
413	7.18	8.15	1105	30.22	-1.00
423	6.90	7.79	1056	28.85	-1.00

Table 4.7 Experimental results for PRF 50

Inlet gas temperature (K)	Compression ratio	Calculated compression ratio	Calculated DCR	Pressure (bar)	CAD
313	7.69	8.85	1183	23.79	-1.00
323	7.84	9.04	1204	25.00	-1.00
333	7.79	9.00	1197	25.68	-1.00
343	7.78	8.99	1196	27.38	-1.00
353	7.62	8.78	1173	27.15	-1.00
363	7.70	8.86	1185	28.52	-1.00
373	7.75	8.92	1192	32.66	-1.00
383	7.72	8.91	1188	31.06	-1.00
393	7.80	9.05	1199	31.28	-1.00
403	7.35	8.38	1133	32.90	-1.00
413	7.43	8.50	1145	31.31	-1.00
423	6.83	7.61	1043	27.30	-1.00

Table 4.8 Experimental results for PRF 60

Inlet gas temperature (K)	Compression ratio	Calculated compression ratio	Calculated DCR	Pressure (bar)	CAD
313	8.32	9.65	1265	28.08	-1.00
323	8.34	9.66	1267	28.12	-1.00
333	8.35	9.68	1269	28.69	-1.00
343	7.96	9.22	1220	25.52	-1.00
353	7.82	9.05	1201	29.68	-1.00
363	7.87	9.10	1208	29.05	-1.00
373	7.91	9.17	1214	31.56	-1.00
383	8.01	9.29	1227	33.08	-1.00
393	8.19	9.47	1249	33.18	-1.00
403	7.99	9.24	1224	34.43	-1.00
413	7.72	8.91	1188	32.31	-1.00
423	7.76	8.95	1193	34.50	-1.00

Table 4.9 Experimental results for PRF 70

Inlet gas temperature (K)	Compression ratio	Calculated compression ratio	Calculated DCR	Pressure (bar)	CAD
313	8.94	10.34	1333	29.72	-1.00
323	8.41	9.76	1276	27.42	-1.00
333	8.64	10.02	1301	28.50	-1.00
343	8.63	10.01	1300	31.32	-1.00
353	8.53	9.89	1289	31.90	-1.00
363	8.64	10.02	1301	34.55	-1.00
373	8.52	9.88	1288	36.58	-1.00
383	8.62	9.95	1299	35.82	-1.00
393	7.78	8.97	1196	32.93	-1.00
403	7.81	9.02	1200	34.37	-1.00
413	8.54	9.89	1290	35.91	-1.00
423	8.59	9.95	1296	35.25	-1.00

Table 4.10 Experimental results for PRF 80

Inlet gas temperature (K)	Compression ratio	Calculated compression ratio	Calculated DCR	Pressure (bar)	CAD
313	9.44	10.83	1380	33.38	-1.00
323	9.11	10.47	1349	30.90	-1.00
333	9.19	10.57	1357	33.07	-1.00
343	9.17	10.55	1355	32.97	-1.00
353	9.11	10.47	1349	36.72	-1.00
363	9.20	10.59	1358	37.90	-1.00
373	9.27	10.68	1365	39.80	-1.00
383	9.31	10.67	1368	37.86	-1.00
393	9.58	10.93	1392	37.51	-1.00
403	9.24	10.65	1362	37.79	-1.00
413	9.46	10.84	1382	35.79	-1.00
423	9.48	10.85	1384	35.27	-1.00

Table 4.11 Experimental results for PRF 90

Inlet gas temperature (K)	Compression ratio	Calculated compression ratio	Calculated DCR	Pressure (bar)	CAD
313	10.31	11.55	1450	37.09	-1.00
323	10.61	11.81	1472	39.38	-1.00
333	10.48	11.71	1462	40.59	-1.00
343	9.55	10.94	1390	36.38	-1.00
353	9.53	10.91	1388	38.35	-1.00
363	9.81	11.16	1412	40.24	-1.00
373	9.40	10.79	1376	40.63	-1.00
383	10.24	11.53	1445	41.16	-1.00
393	10.36	11.64	1454	38.66	-1.00
403	9.43	10.82	1379	41.14	-1.00
413	10.29	11.58	1449	35.58	-1.00
423	10.26	11.57	1447	33.96	-1.00

Generally, in the experiments, the difference between the calculated compression ratio and that of the control program, increase with increased compression ratio due to the exponential behavior of the correct compression ratio.

The compression ratio decreases with increased inlet temperature, which is clearly seen with the lower PRFs. On the other hand, with the higher PRFs there is only a very slight difference in compression ratio.

Concerning the ignition pressure, the variation is too big for a trend to be spotted.

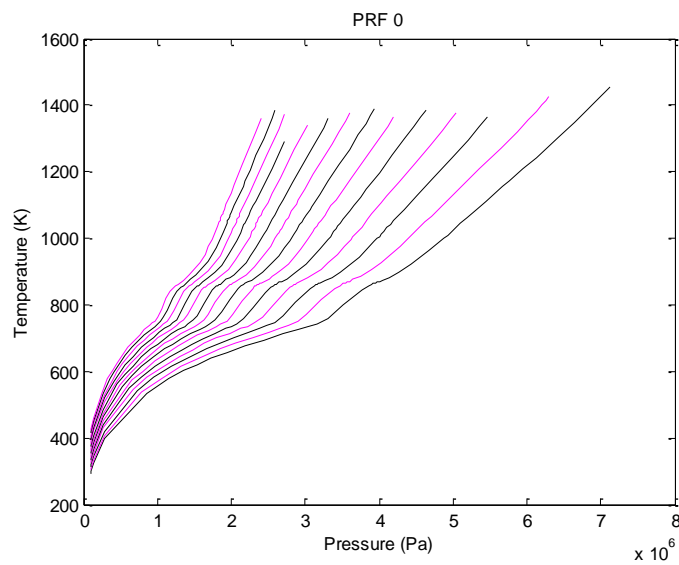
4.2 Results from simulations

With the simulation program the heat release rate, the temperature trace and the pressure trace were obtained. To be able to determine the ignition temperature with corresponding pressure the heat release rate needed to be accumulated. This was accomplished by the use of Excel, and from the heat release the CAD used to set the ignition temperature with corresponding pressure, was determined. The results from the simulations are presented below.

The results for PRF 0 are shown in table 4.12. The data is plotted in Matlab, see figure 4.2.

Table 4.12 The results for PRF 0

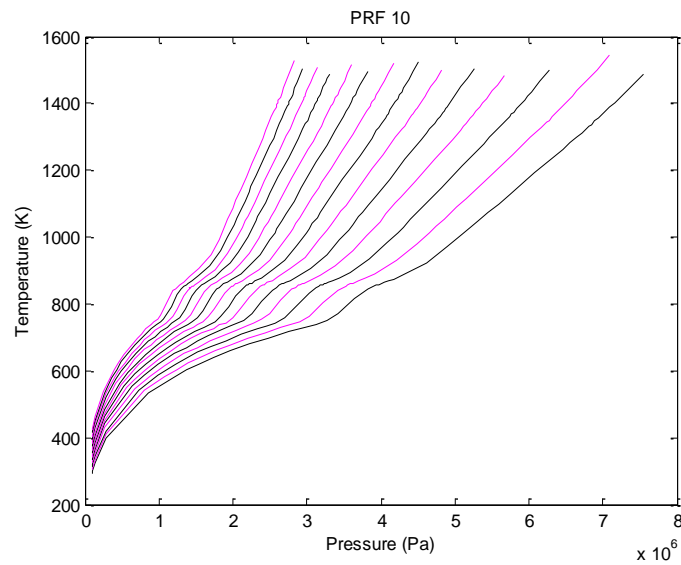
Inlet gas temp (K)	Compression ratio	Ignition temp (K)	Ignition pressure (bar)	CAD
293	13.78	971	47.17	-1.53
303	12.85	959	41.98	-1.75
313	12.00	966	38.24	-1.56
323	11.30	960	34.67	-1.85
333	10.66	966	31.93	-1.83
343	10.07	972	29.48	-1.72
353	9.57	984	27.56	-1.72
363	9.09	981	25.39	-1.79
373	8.67	989	23.77	-1.70
383	8.27	993	22.18	-1.51
393	7.92	1002	20.90	-1.23
403	7.65	1004	19.70	-1.63
413	7.39	1011	18.70	-1.69
423	7.13	1011	17.64	-1.49

**Figure 4.2 The results for PRF 0**

The results for PRF 10 are shown in table 4.13. The data is plotted in Matlab, see figure 4.3.

Table 4.13 The results for PRF 10

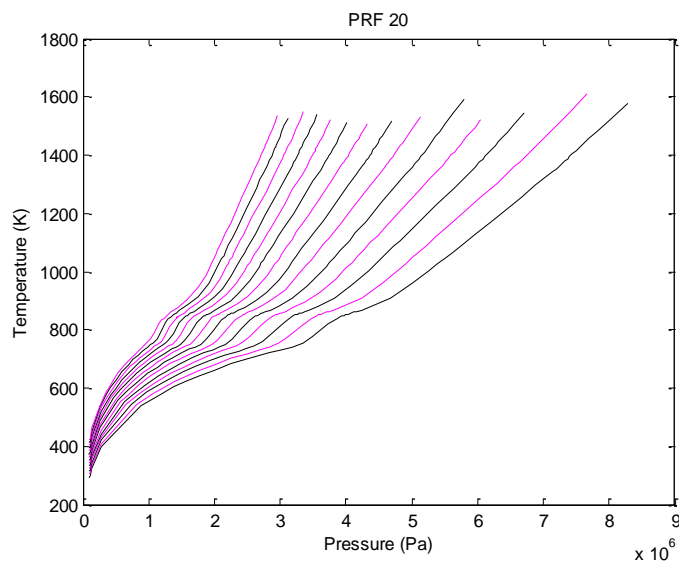
Inlet gas temp (K)	Compression ratio	Temperature (K)	Pressure (bar)	CAD
293	14.3	1003	50.68	-1.14
303	13.43	1006	46.13	-1.39
313	12.6	1002	42.54	-1.27
323	11.85	1003	38.04	-1.51
333	11.2	1013	35.57	-1.45
343	10.6	1032	33.04	-1.43
353	10.07	1054	31.19	-1.38
363	9.59	1031	28.17	-1.79
373	9.13	1020	25.82	-1.89
383	8.75	1077	25.53	-1.50
393	8.36	1076	23.76	-1.29
403	8.05	1064	22.02	-1.58
413	7.75	1058	20.57	-1.62
423	7.5	1059	19.44	-1.79

**Figure 4.3 The results for PRF 10**

The results for PRF 20 are shown in table 4.14. The data is plotted in Matlab, see figure 4.4.

Table 4.14 The results for PRF 20

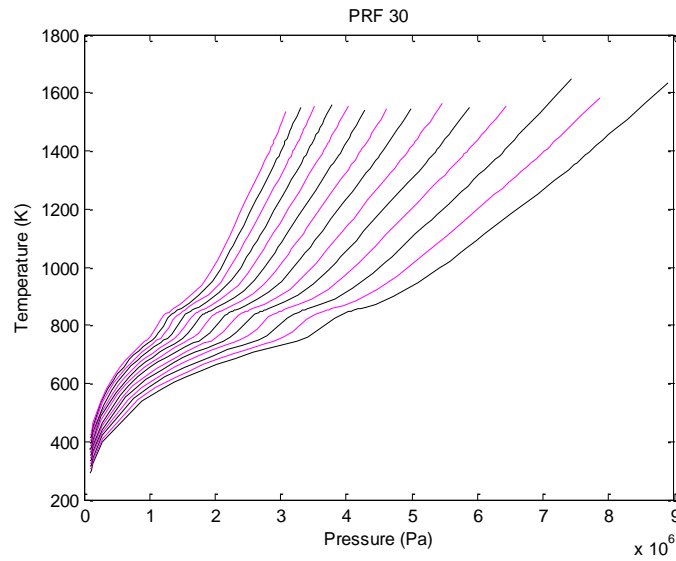
Inlet gas temp (K)	Compression ratio	Temperature (K)	Pressure (bar)	CAD
293	14.85	999	52.35	-1.20
303	13.96	1015	48.40	-1.26
313	13.1	1019	44.14	-1.19
323	12.35	1034	40.96	-1.14
333	11.7	1036	37.71	-1.38
343	11.05	1054	35.22	-1.12
353	10.5	1048	32.30	-1.31
363	9.99	1027	29.24	-1.61
373	9.53	1034	27.33	-1.62
383	9.12	1044	25.74	-1.62
393	8.74	1103	25.49	-1.16
403	8.40	1068	23.07	-1.52
413	8.08	1097	22.28	-1.23
423	7.807	1105	21.17	-1.27

**Figure 4.4 The results for PRF 20**

The results for PRF 30 are shown in table 4.15. The data is plotted in Matlab, see figure 4.5.

Table 4.15 The results for PRF 30

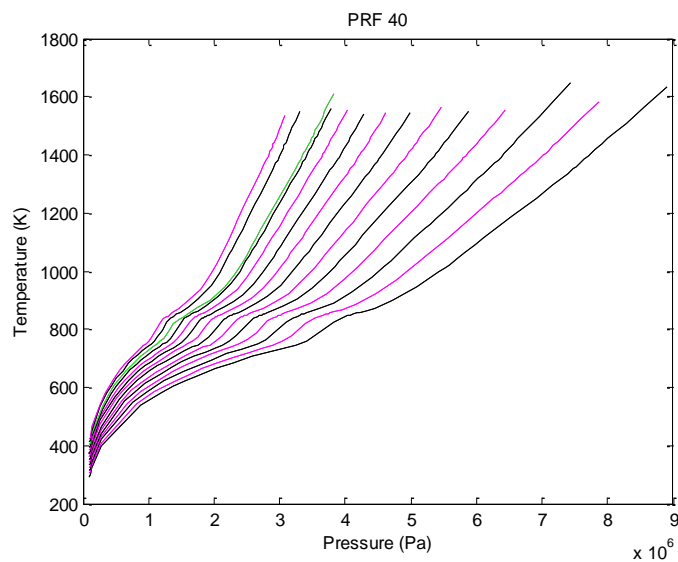
Inlet gas temp (K)	Compression ratio	Temperature (K)	Pressure (bar)	CAD
293	15.45	1002	54.62	-1.18
303	14.51	1009	49.99	-1.20
313	13.67	1006	45.39	-1.41
323	12.88	1025	42.31	-1.16
333	12.18	1040	39.43	-1.08
343	11.57	1044	36.50	-1.26
353	10.97	1043	33.56	-1.22
363	10.45	1061	31.67	-1.15
373	9.97	1077	29.88	-1.08
383	9.53	1084	27.98	-1.06
393	9.15	1067	25.74	-1.40
403	8.78	1092	24.70	-1.17
413	8.45	1084	23.01	-1.28
423	8.15	1106	22.12	-1.11

**Figure 4.5 The results for PRF 30**

The results for PRF 40 are shown in table 4.16. The data is plotted in Matlab, see figure 4.6. The curve for the inlet temperature 403 K is marked green in the figure as it differs from its expected appearance. By some unknown reason the simulation program behaves in an unpredictable way in this particular circumstance.

Table 4.16 The results for PRF 40

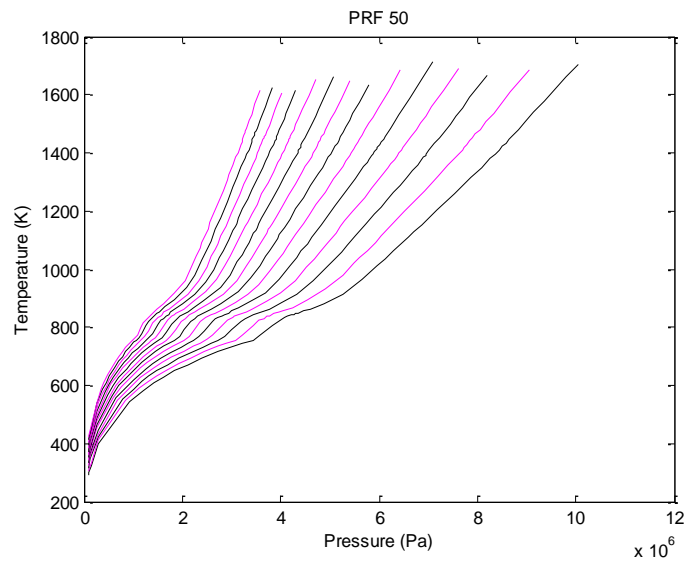
Inlet gas temp (K)	Compression ratio	Temperature (K)	Pressure (bar)	CAD
293	16.07	1009	57.21	-1.05
303	15.12	1016	52.42	-1.08
313	14.24	1023	48.15	-1.02
323	13.46	1017	43.79	-1.21
333	12.75	1034	40.98	-1.12
343	12.10	1042	38.08	-1.12
353	11.51	1041	35.13	-1.24
363	10.96	1063	33.27	-1.07
373	10.46	1052	30.54	-1.23
383	10.00	1056	28.53	-1.23
393	9.59	1054	26.60	-1.37
403	9.22	1089	25.84	-1.16
413	8.87	1081	24.05	-1.26
423	8.55	1105	23.18	-1.05

**Figure 4.6 The results for PRF 40**

The results for PRF 50 are shown in table 4.17. The data is plotted in Matlab, see figure 4.7.

Table 4.17 The results for PRF 50

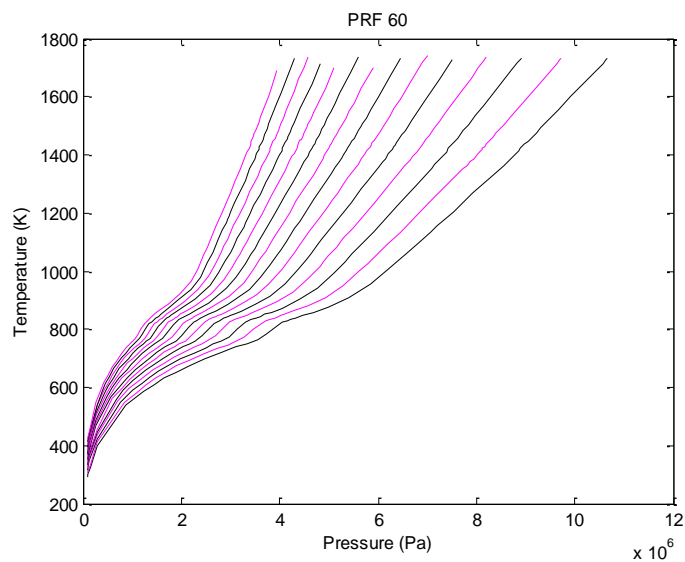
Inlet gas temp (K)	Compression ratio	Temperature (K)	Pressure (bar)	CAD
293	16.75	998	58.86	-1.16
303	15.78	1017	54.72	-1.00
313	14.90	1008	49.54	-1.20
323	14.11	1016	45.83	-1.25
333	13.38	1038	43.17	-1.08
343	12.70	1022	39.05	-1.34
353	12.09	1030	36.45	-1.32
363	11.53	1031	33.80	-1.42
373	11.02	1034	31.54	-1.49
383	10.54	1046	29.76	-1.35
393	10.10	1049	27.85	-1.37
403	9.71	1085	27.08	-1.09
413	9.35	1073	25.14	-1.29
423	9.01	1097	24.23	-1.04

**Figure 4.7 The results for PRF 50**

The results for PRF 60 are shown in table 4.18. The data is plotted in Matlab, see figure 4.8.

Table 4.18 The results for PRF 60

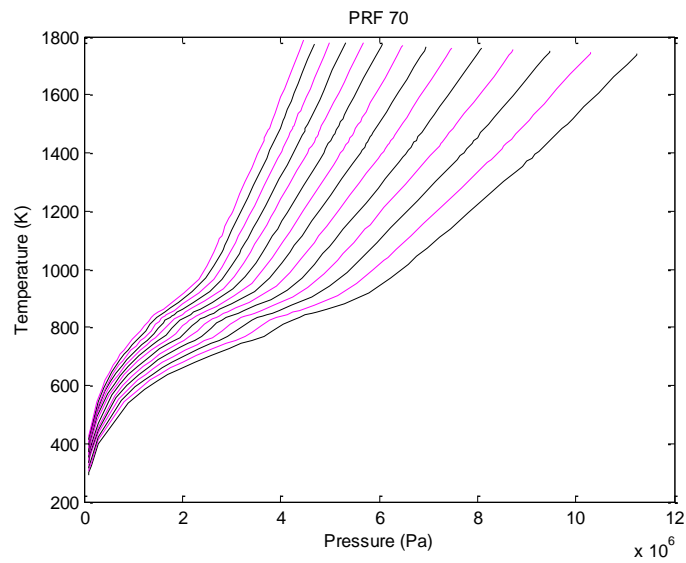
Inlet gas temp (K)	Compression ratio	Temperature (K)	Pressure (bar)	CAD
293	17.52	1003	61.87	-1.08
303	16.525	1014	57.12	-1.01
313	15.63	1022	52.73	-1.03
323	14.81	1027	48.63	-1.04
333	14.06	1032	45.00	-1.07
343	13.38	1027	41.33	-1.26
353	12.75	1049	39.17	-1.06
363	12.17	1049	36.36	-1.12
373	11.64	1057	34.10	-1.12
383	11.15	1072	32.29	-1.05
393	10.70	1064	29.95	-1.19
403	10.29	1083	28.62	-1.10
413	9.908	1062	26.30	-1.37
423	9.56	1088	25.45	-1.13

**Figure 4.8 The results for PRF 60**

The results for PRF 70 are shown in table 4.19. The data is plotted in Matlab, see figure 4.9.

Table 4.19 The results for PRF 70

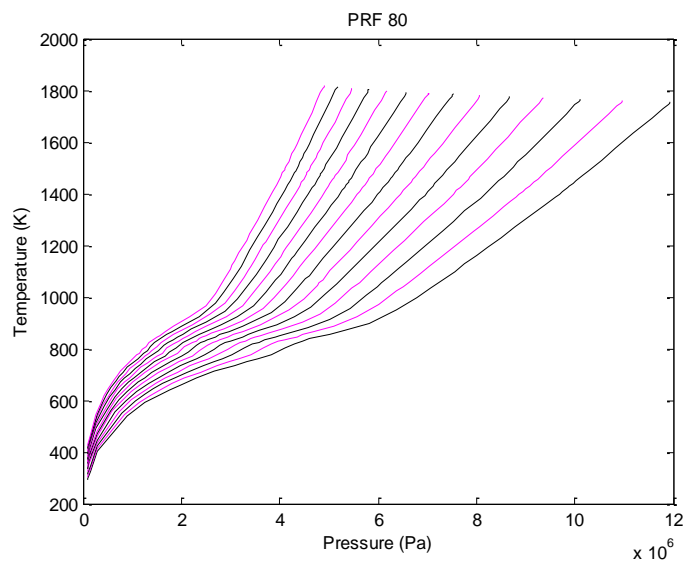
Inlet gas temp (K)	Compression ratio	Temperature (K)	Pressure (bar)	CAD
293	18.38	1003	64.80	-1.11
303	17.37	1012	59.81	-1.04
313	16.45	1019	55.27	-1.03
323	15.62	1026	51.19	-1.04
333	14.86	1029	47.36	-1.10
343	14.16	1033	44.02	-1.12
353	13.51	1049	41.48	-1.01
363	12.92	1054	38.77	-1.04
373	12.37	1057	36.21	-1.06
383	11.87	1059	33.30	-1.13
393	11.40	1067	31.98	-1.09
403	10.98	1079	30.40	-1.10
413	10.58	1081	28.61	-1.10
423	10.22	1065	26.51	-1.39

**Figure 4.9 The results for PRF 70**

The results for PRF 80 are shown in table 4.20. The data is plotted in Matlab, see figure 4.10.

Table 4.20 The results for PRF 80

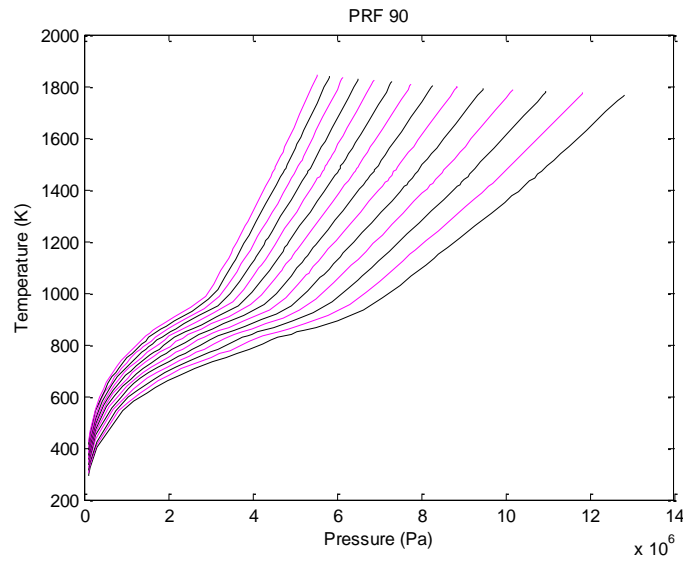
Inlet gas temp (K)	Compression ratio	Temperature (K)	Pressure (bar)	CAD
293	19.37	994	67.56	-1.14
303	18.36	1009	62.94	-1.09
313	17.43	1015	58.20	-1.04
323	16.59	1022	54.08	-1.09
333	15.82	1030	50.43	-1.07
343	15.105	1036	47.02	-1.09
353	14.45	1042	43.96	-1.06
363	13.84	1049	41.26	-1.02
373	13.28	1052	38.58	-1.12
383	12.77	1060	36.45	-1.13
393	12.29	1063	34.28	-1.16
403	11.848	1072	32.51	-1.10
413	11.44	1072	30.06	-1.12
423	11.07	1089	29.41	-1.04

**Figure 4.10 The results for PRF 80**

The results for PRF 90 are shown in table 4.21. The data is plotted in Matlab, see figure 4.11.

Table 4.21 The results for PRF 90

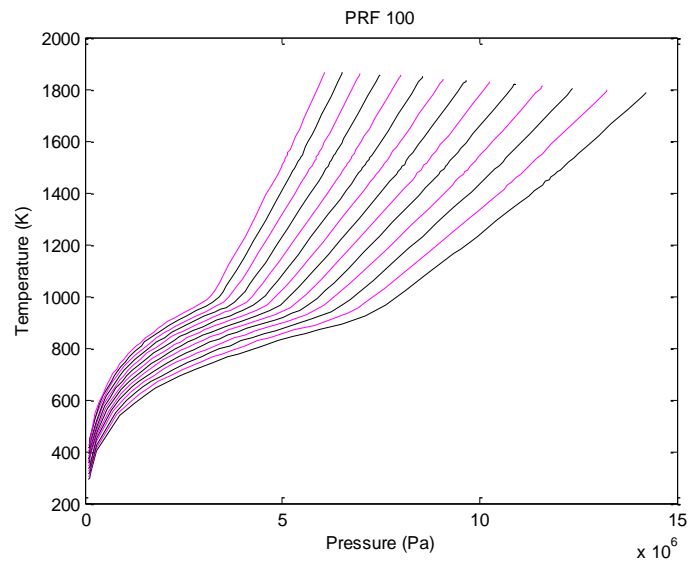
Inlet gas temp (K)	Compression ratio	Temperature (K)	Pressure (bar)	CAD
293	20.64	999	72.34	-1.07
303	19.63	1003	66.78	-1.07
313	18.71	1014	62.32	-1.04
323	17.86	1022	58.14	-1.08
333	17.09	1022	53.90	-1.12
343	16.38	1026	50.34	-1.18
353	15.73	1040	47.67	-1.16
363	15.12	1043	44.67	-1.16
373	14.56	1046	41.98	-1.18
383	14.04	1058	39.91	-1.06
393	13.56	1058	37.52	-1.16
403	13.11	1069	35.76	-1.12
413	12.695	1081	34.19	-1.01
423	12.315	1077	32.20	-1.15

**Figure 4.11 The results for PRF 90**

The results for PRF 100 are shown in table 4.22. The data is plotted in Matlab, see figure 4.12.

Table 4.22 Results for PRF 100

Inlet gas temp (K)	Compression ratio	Temperature (K)	Pressure (bar)	CAD
293	22.63	1003	79.46	-1.06
303	21.68	1002	73.46	-1.06
313	20.83	1009	68.87	-1.06
323	20.06	1018	64.82	-1.06
333	19.35	1022	60.89	-1.04
343	18.69	1038	58.05	-1.06
353	18.04	1036	54.25	-1.04
363	17.39	1041	51.10	-1.02
373	16.74	1048	48.20	-1.07
383	16.06	1053	45.27	-1.03
393	15.37	1061	42.57	-1.04
403	14.68	1065	39.80	-1.00
413	14.02	1071	37.29	-1.02
423	13.38	1078	34.99	-1.00

**Figure 4.12 The results for PRF 100**

As in the experiments, the compression ratio decreases with increased inlet temperature. The pressure also decreases with increasing inlet temperature, which is opposite to the behavior in the experiments.

5. Conclusions

In this chapter the results are discussed in detail and conclusions from this master thesis are presented.

5.1 Discussion

The results from the simulations seem to be reasonable. The compression ratios and the ignition temperatures with the corresponding pressures are in the right magnitude. Although the model is homogenous the results obtained are relatively good, but the pressure tends to be a bit too high.

The results from the experiments, on the other hand, are not as reliable as the results from the simulations. The compression ratio has the same trend as in the simulations, which is positive, but the value is much lower. The correct compression ratio lies probably around the value obtained from the simulations. The ignition pressures from the experiments are probably not correct. Most of the values are unreasonable; furthermore a trend in the results could not be spotted.

The values from the simulations and the experiments differ a lot. To explore the possible reasons for this deviation simulations and experiments for PRF 50 with an inlet gas temperature of 363 K were compared. The blue curve is the simulated values and the red curve is the experimental values.

The accumulated heat release in the simulations and the experiments are almost the same, 585 J and 539 J respectively. In figure 5.1, the heat release rate is compared to each other. As seen in figure 5.1, the reaction rate is not the same in the simulations as in the experiments, due to the homogenous model. The reaction rate and possibly the side reactions that are not included in the chemical model could also affect this behavior.

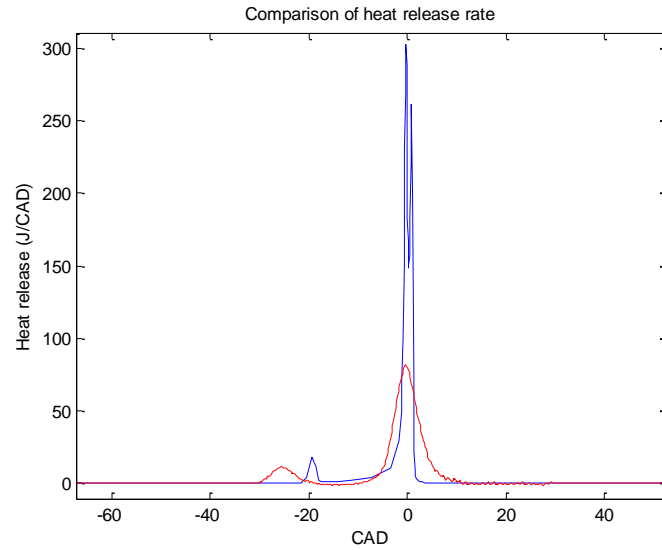


Figure 5.1 Comparison of heat release rate

In figure 5.2, the pressure traces are compared to each other. The low pressure at the intake valve closing in the experiments is not the same as in the simulations, see figure 5.2. The deviation escalates with the increasing pressure, resulting in a significant error. This error can be corrected by calibration of the pressure in the CFR engine.

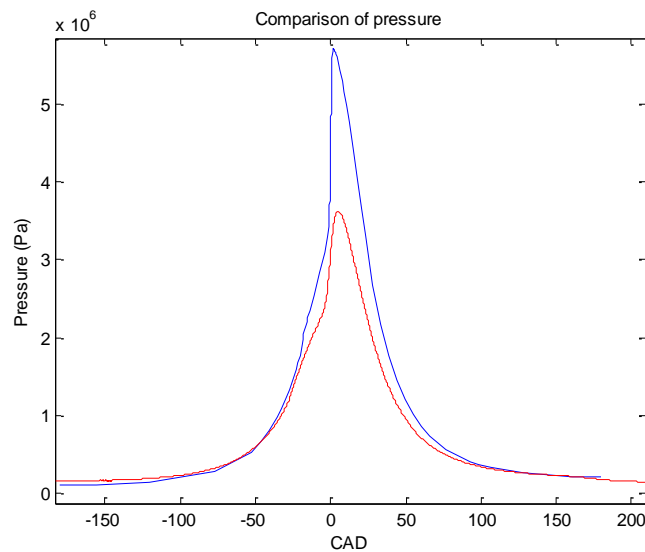


Figure 5.2 Comparison of pressure trace

In figure 5.3, the CAD for the intake valve closing is determined. In the graph the conditions are the same in the simulations and the experiments. The compression ratio is that of the experiments, i.e. the calculated value 8.86. The CAD for the intake valve closing was determined to -120° , i.e. 60° ABDC, which differs a lot from the intake valve closing used in the simulations, which was

-180°. While comparing figure 5.2 and 5.3 a remarkable difference is seen. In figure 5.2 the blue curve is much higher than the red curve, but in figure 5.3 the behavior is the opposite. In the figures the impact of the IVC is shown; in figure 5.2 it is -180° and in figure 5.3 it is -120°.

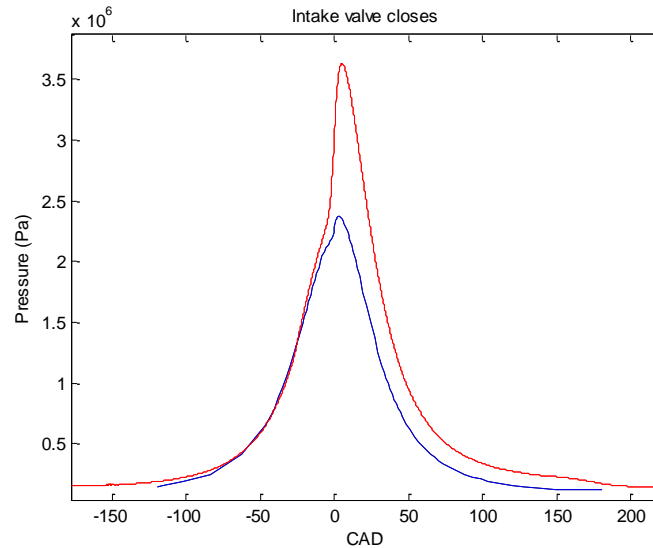


Figure 5.3 Determination of the CAD for intake valve closing

In order to examine the impact of the intake valve closing the simulation was executed with the new values. The difference in compression ratio between the experiments and the simulations has increased from 11.53 to 13.50.

One of the reasons why the simulated values are a lot higher than the experimental ones might be that the simulations were not executed at the right intake valve closing. The residual gases are set to 10 percent in the simulations but this is only a set value that might attribute to the difference. Another reason might be that the temperature indicator on the CFR engine was placed incorrectly.

5.2 Conclusions

A good way to compare combustion of fuels in different engines is to develop a fuel index. In a fuel index data for mixtures are accounted for in a table, with which the index of an unknown fuel can be determined. To define an HCCI fuel index several different fuels must be tested. In order to start developing an HCCI index, PRF 0 – 100 was simulated with DARS and experiments with the CFR engine was executed.

In the experiments, the lowest inlet gas temperature obtained was 303 K and therefore the inlet temperatures 293 K and 303 K could only be simulated in DARS. The fuel PRF 100 was not able to be run in the CFR engine due to its too high compression ratio.

The simulated data may be used in further development of an HCCI index. The model created in this master thesis may be used with an engine that has the same conditions as the simulations, if a more accurate chemical model is used and the indicator for the inlet temperature is placed at the correct location. This way of reasoning also implies to the relation between the accurate compression ratio and the digital counter reading that was established in this master thesis.

In the figures presented in this thesis it is shown that the more iso-octane in the mixture the less cool flame combustion present. The type of tables and figures presented in this master thesis can be used to determine the optimal compression ratio and octane number for a fuel mixture.

Further research concerning the reason why the simulations and the experiments deviated is needed in order to be able to use this base for an index.

6. References

- [1] Johansson, Bengt, 2003, *Förbränningsmotorer del 1 och 2*, Division of Combustion Engines, Department of Heat and Power Engineering, Lund Institute of Technology

- [2] Eastop, T.D. and McConkey, A, 1993, *Applied Thermodynamics for Engineering Technologists*, Pearson Prentice Hall, 5th edition, p. 176-183, 16, 88

- [3] Danielsson, Nils-Åke, 2006, *Kemisk Reaktionsteknik A*, Institute of chemical engineering, Lund Institute of Technology, 2nd edition

- [4] Waukesha CFR, 2003, *F-1 & F-2 Research method (F-1), Motor method (F-2), Octane rating units, Operation & maintenance*, Dresser Inc, 2nd edition, p. 2.05-1 – 2.05-9

- [5] Tsurushima, T, 2009, *A new skeletal PRF kinetic model for HCCI combustion*, Proceedings of the Combustion Institute, Volume 32, Number 2

- [6] Heywood, John B, 1988, *Internal Combustion Engine Fundamentals*, McGraw-Hill, p. 680

- [7] Personal communication with Professor Bengt Johansson, September 20 2008

Appendix – Raw data from the experiments

Date: 10/12 2008

Table 1. Inlet temperature: 423 K

Fuel	Compression ratio
PRF 0	5.79
	5.74
PRF 10	6.00
	5.84
PRF 20	6.10
	6.06
PRF 30	6.34
	6.38
PRF 40	6.82
	6.76
PRF 50	7.08
	7.18
PRF 60	7.70
	7.62
PRF 70	8.57
	8.46
PRF 80	9.55
	9.46
PRF 90	10.40
	10.33

B

Table 2. Inlet temperature: 413 K

Fuel	Compression ratio
PRF 0	6.52
	6.08
PRF 10	6.19
	6.02
PRF 20	6.27
	6.14
PRF 30	6.53
	6.47
PRF 40	7.15
	6.91
PRF 50	7.34
	7.23
PRF 60	7.67
	7.62
PRF 70	8.54
	8.40
PRF 80	9.52
	9.39
PRF 90	10.48
	10.32

Date: 15/12 2008

Table 3. Inlet temperature: 403 K

Fuel	Compression ratio
PRF 0	6.29
	6.4
PRF 10	6.29
	6.18
PRF 20	6.3
PRF 30	6.36
	6.62
PRF 40	6.98
	6.91
PRF 50	7.23
	7.20
PRF 60	7.58
	7.66
PRF 70	8.45
	8.45
PRF 80	9.30
	9.36
PRF 90	10.33

D

Table 4. Inlet temperature: 393 K

Fuel	Compression ratio
PRF 0	6.31
	6.27
PRF 10	6.54
	6.44
PRF 20	6.73
	6.68
PRF 30	7.12
	7.07
PRF 40	7.37
	7.51
PRF 50	7.67
	7.76
PRF 60	8.11
	8.03
PRF 70	8.75
	8.75
PRF 80	9.64
	9.45
PRF 90	10.58
	10.46

Table 5. Inlet temperature: 383 K

Fuel	Compression ratio
PRF 0	6.54
	6.48
PRF 10	6.71
	6.65
PRF 20	6.93
	6.85
PRF 30	6.95
	7.17
PRF 40	7.14
	7.33
PRF 50	7.60
	7.72
PRF 60	7.97
	7.92
PRF 70	8.50
	8.65
PRF 80	9.29
	9.48
PRF 90	10.50
	10.33

F

Date: 29/1 2009

Table 6. Inlet temperature: 373 K

Fuel	Compression ratio
PRF 0	6.72
	6.63
PRF 10	6.69
	6.81
PRF 20	6.85
	6.95
PRF 30	7.04
	7.14
PRF 40	7.33
	7.41
PRF 50	7.58
	7.70
PRF 60	7.88
	7.99
PRF 70	8.54
	8.69
PRF 80	9.27
	9.37
PRF 90	9.96
	10.08

Table 7. Inlet temperature: 363 K

Fuel	Compression ratio
PRF 0	6.94
	7.01
PRF 10	7.03
	6.94
PRF 20	7.01
	7.14
PRF 30	7.14
	7.26
PRF 40	7.44
	7.55
PRF 50	7.70
	7.79
PRF 60	7.95
	8.05
PRF 70	8.62
	8.79
PRF 80	9.18
	9.37
PRF 90	10.03
	9.81

Table 8. Running without combustion, with an inlet temperature of 325 K

Digital counter reading	Number
0	145232
100	145455
200	145647
300	145942
400	150148
500	150343
600	150546

Date: 30/1 2009

H

Table 9. Inlet temperature: 353 K

Fuel	Compression ratio
PRF 0	7.14
	7.21
PRF 10	7.09
	7.15
PRF 20	7.15
	7.23
PRF 30	7.33
	7.26
PRF 40	7.47
	7.53
PRF 50	7.67
	7.79
PRF 60	7.99
	8.06
PRF 70	8.65
	8.79
PRF 80	9.20
	9.29
PRF 90	9.59
	9.79

Table 10. Inlet temperature: 343 K

Fuel	Compression ratio
PRF 0	7.65
	7.71
PRF 10	7.54
	7.62
PRF 20	7.57
	7.65
PRF 30	7.65
	7.71
PRF 40	7.84
	7.90
PRF 50	8.00
	8.14
PRF 60	8.24
	8.32
PRF 70	8.89
	9.02
PRF 80	9.34
	9.53
PRF 90	9.78
	9.59

J

Date: 3/2 2009

Table 9. Inlet temperature: 333 K

Fuel	Compression ratio
PRF 0	7.84
	7.91
PRF 10	7.71
	7.62
PRF 20	7.69
	7.76
PRF 30	7.79
	7.93
PRF 40	8.03
	8.14
PRF 50	8.35
	8.42
PRF 60	8.69
	8.81
PRF 70	8.94
	9.02
PRF 80	9.43
	9.47
PRF 90	10.73
	10.95

Table 12. Inlet temperature: 323 K

Fuel	Compression ratio
PRF 0	8.30
	8.38
PRF 10	8.01
	7.82
PRF 20	7.88
	7.99
PRF 30	7.99
	8.13
PRF 40	8.23
	8.39
PRF 50	8.51
	8.63
PRF 60	8.84
	8.97
PRF 70	9.11
	9.25
PRF 80	9.64
	9.74
PRF 90	10.78
	10.91

L

Table 10. Inlet temperature: 313 K

Fuel	Compression ratio
PRF 0	7.96
	8.15
PRF 10	8.02
	8.11
PRF 20	8.01
	8.22
PRF 30	8.22
	8.41
PRF 40	8.45
	8.64
PRF 50	8.80
	8.89
PRF 60	9.11
	9.25
PRF 70	9.35
	9.39
PRF 80	9.84
	9.90
PRF 90	10.69
	10.88

Table 11. Rerunning of tests

Fuel	Compression ratio
PRF 0 – 383 K	6.69
	6.73
PRF 0 – 413 K	6.24
	6.30
PRF 10 – 383 K	6.75
	6.64
PRF 20 – 403 K	6.35
	6.29
PRF 30 – 393 K	6.64
	6.71
PRF 50 – 423 K	6.83
	6.89
PRF 70 – 393 K	7.78
	7.88
PRF 70 – 403 K	7.64
	7.76
PRF 90 – 403 K	9.32
	9.49

Date: 17/2 2009

Table 12. Rerunning of tests

Fuel	Compression ratio
PRF 0 – 333 K	7.33
	7.41
PRF 0 – 363 K	6.78
	6.85
PRF 0 – 413 K	5.92
	6.03
PRF 10 – 343 K	7.32
	7.40
PRF 20 – 333 K	7.53
	7.62
PRF 20 – 343 K	7.40
	7.32
PRF 20 – 353 K	7.08
	7.16
PRF 20 – 363 K	6.87
	6.96
PRF 20 – 373 K	6.69
	6.77
PRF 30 – 353 K	7.31
	7.40
PRF 30 – 373 K	6.85
	6.70
PRF 40 – 333 K	7.97
	8.07
PRF 40 – 343 K	7.71
	7.83
PRF 40 – 353 K	7.34
	7.60

Table 13. Rerunning of tests

Fuel	Compression ratio
PRF 40 – 363 K	7.31

	7.43
PRF 60 – 343 K	8.29
	8.40
PRF 70 – 323 K	8.89
	9.01
PRF 80 – 323 K	9.38
	9.48
PRF 90 – 343 K	9.59
	9.82
PRF 90 – 373 K	9.34
	9.47
